2008

Fin-and-Tube Heat Exchanger Solid Core Advanced Simulation

Carles Oliet
Technical University of Catalonia

Carlos D. Perez-Segarra
Technical University of Catalonia

Jesus Castro
Technical University of Catalonia

Assensi Oliva
Technical University of Catalonia

Fin-and-Tube Heat Exchanger Solid Core Advanced Simulation

Carles OLIET*, Carlos D. PEREZ-SEGARRA, Jesus CASTRO, Assensi OLIVA

Centre Tecnològic de Transferència de Calor (CTTC),
Universitat Politècnica de Catalunya (UPC),
ETSEIAT, C.Colom 11, 08222 Terrassa (Barcelona), Spain
Tel. +34-93-7398192, Fax: +34-93-7398920
cttc@cttc.upc.edu, http://www.cttc.upc.edu

ABSTRACT

This paper is devoted to the presentation of an advanced model for the heat conduction processes within a finned tube bundle, typically found in air-cooled evaporators and condensers. As a result of the computational effort needed to simulate the desired fin-and-tube local unsteadiness, some actions have been undertaken in order to obtain reasonable simulation time consumption. A specific cutting cell grid has been proposed for the fins to adapt to the tubes shape, reducing strongly the grid density comparing to alternative methods such as the blocking-off. Additionally, a specific numerical procedure has been formulated to maintain the matrix of coefficients constant, allowing the use of direct solvers for the system of equations. Another important aspect of the current approach is the angular discretisation of the tubes, oriented to take into account angular variations of in-tube heat transfer coefficients (as in stratified flow, typical of liquid overfeed evaporators). Verification studies are presented based on MMS methodology. Some illustrative results are also presented regarding transient simulations of finned tube evaporators and an initial study of the influence of in-tube heat transfer coefficient asymmetry.

1. INTRODUCTION

This paper is devoted to the presentation of a new numerical strategy to simulate the expanded fin-and-tube solid core, typically formed by a finned round tube bank and found in numerous equipment such as air-cooled condensers, evaporators, automotive radiators, etc.

The main objective is the transient and local evaluation of the temperature in the fin-and-tube core, considering internal distributed heat transfer coefficient. This goal is related to the development of a future tool, based on previous models by the authors, on liquid overfeed evaporators, that will deal with transient processes of frosting and defrosting, stratified intube two-phase flow, airflow maldistribution, etc. and their impact on refrigerated chambers behaviour. Previous developed fin-and-tube heat exchanger numerical model ((Oliet et al., 2002), (Pérez-Segarra et al., 2006b)), is being improved from the point of view of the solid simulation in order to allow pure transient simulation of the tubes and fins.

Some recent works have been identified in the published literature on the calculation of plain transversal fins around tubes. In (Hoffenbecker et al., 2005) an interesting model was presented for unsteady circular fin simulation, including frost. The proposed discretisation is axysymmetric and assumes adiabatic fin edge for each tube. A bi-dimensional simulation was presented in (Liang et al., 2000) for steady state, centering the work in a comparison of the effects of several assumptions (1D/2D, air distribution properties, rectangular/circular) on the fin efficiency. (Sommers and Jacobi, 2006) analysed analytically a two-dimensional frost layer onto a one-dimensional circular fin, obtaining the corresponding fin efficiency.

In previous versions of the model the fin was evaluated either by using fin efficiency concept or by doing a 2D steady heat conduction simulation to detect possible transversal heat transfer bridges between tubes at different temperature. If full transient simulation of the fin-and-tube core is desired, the fins must be analysed independently by applying fundamental heat transfer procedures, at each time step. In order to reduce the computational time consumption, the fin discretisation has been generated ex-professo adapting the cartesian cells to the tube shape when necessary. Previous approaches as the "blocking-off" method demanded too dense grids. It should be noticed at this point that an automatic mesh generation is desired

in the heat exchanger model. Other actions such as the use of appropriate solvers for the set of equations have also been considered.
Another important innovation of the presented model is the coupling of the fin simulation with the simulation of the tubes in cylindrical co-ordinates (axial and angular discretisation), being both grids independent. The angular analysis of the tube heat conduction allows the study of situations where the internal heat transfer coefficient shows important asymmetries (e.g. stratified flow in liquid overfeed evaporators).

2. MATHEMATICAL FORMULATION - NUMERICAL PROCEDURE

The mathematical formulation of this problem, as being the study of the solid elements in the fin-and-tube heat exchanger, is based on the general heat diffusion equation (Eq. 1). The radiative heat transfer contribution has been neglected, and no internal heat sources are considered. External convective heat transfer interactions with the air or liquid flows, are formulated through the Newton's law of cooling.

$$\rho c_p \frac{\partial T}{\partial t} = \nabla \cdot (k \nabla T) + \dot{q}_{conv} \tag{1}$$

2.1 Fin discretized equations

One way to reduce the amount of computational resources needed in the transient simulation of the fins is to reduce the grid density. The discretization approach used previously by the authors was the so-called "blocking-off" method (in-out of the tube area). In order to assure an accurate result, a very fine mesh was required, with the corresponding increase of computational time. The current approach moves to a "cutting cell" method, that is, generating new cells around the tubes which adapt to the tube shape (Figure 1). In order to avoid cells with tangential contact with the tube, an odd number of fin cells (N_f) has been fixed to cover the tube diameter plus an additional fin grid space, that is $\Delta x = D/(N_f - 1)$. From the grid fixed at each tube area, the inter-tube area has been discretized with a grid proportional to that one. Once the Cartesian grid has been generated, the fin cells with nodes inside the tubes are re-generated to follow the tube shape (Figure 1). Different cases appear depending on the number of nodes inside the tube area and the orientation (Figure 1), while if all the fin cell is in the tube area that fin cell is removed.

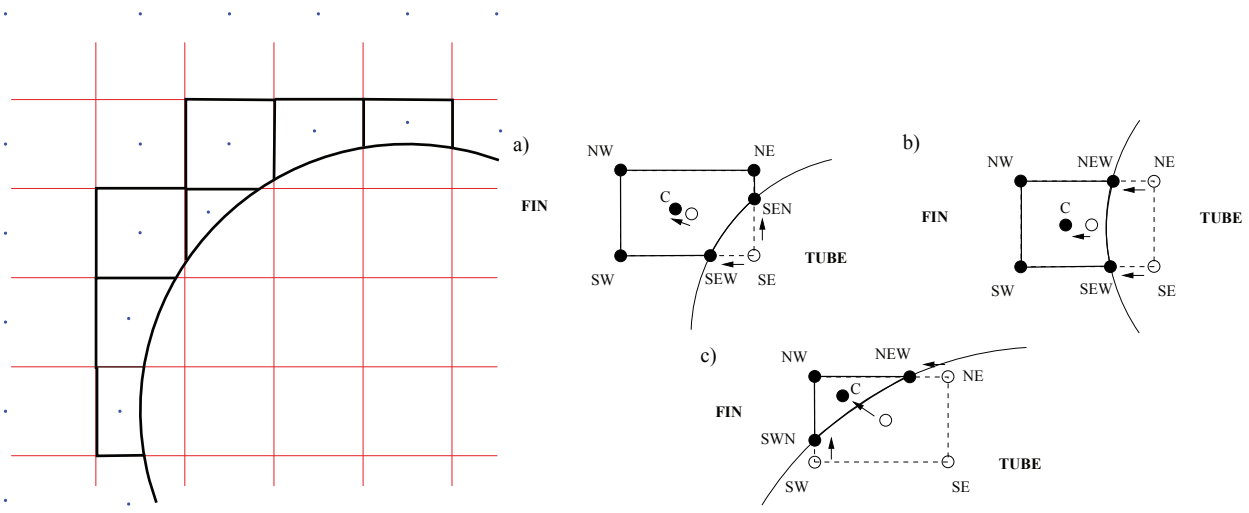

Figure 1: Left: New cutting-cell discretisation scheme. Right: Re-generation of fin cells with tube contact.

The diffusive heat flux through fin cell faces considering non-orthogonality, has been calculated by the following expression (incoming heat) (Pérez-Segarra et al., 2006a) (where $\hat{A}_f = A_f/(\vec{n}_f \cdot \vec{s}_f)$):

$$\dot{Q}_f \approx k_f \frac{(T_F - T_P)}{d_{PF}} \hat{A}_f + k_f \overline{\nabla T}_f \cdot [A_f \vec{n}_f - \hat{A}_f \vec{s}_f] \tag{2}$$

The interpolated gradient at cell face is calculated following the interpolation criteria indicated by (Pérez-Segarra et al., 2006a) from the gradients at cell centroids: $\overline{\nabla T}_f \approx \nabla T_f = (1-\alpha_f)\nabla T_P + \alpha_f \nabla T_F$, where $\alpha_f = (\overrightarrow{Pf} \cdot \vec{s}_f)/(\overrightarrow{PF} \cdot \overrightarrow{PF})^{1/2}$.
Applying the heat diffusion equation stated in Eq.1 to a general fin cell (Figure 2), and considering expression (Eq. 2) for the heat flux through the internal fin cell faces, the corresponding discretized equation is obtained:

$$\rho c_p \frac{aT_P - bT_P^0 + cT_P^{00}}{\Delta t} V = (\dot{Q}_s + \dot{Q}_n + \dot{Q}_w + \dot{Q}_e) + \sum [\frac{\dot{Q}_{b,i}}{n_{F,i} A_{bF,i}} A_i] - \dot{Q}_a \tag{3}$$

$$\begin{aligned} \rho c_p \frac{aT_P - bT_P^0 + cT_P^{00}}{\Delta t} V \;=\; & k_s \frac{T_S - T_P}{d_{PS}} \hat{A}_s + k_n \frac{T_N - T_P}{d_{PN}} \hat{A}_n + k_w \frac{T_W - T_P}{d_{PW}} \hat{A}_w + k_e \frac{T_E - T_P}{d_{PE}} \hat{A}_e + \\ & k_s \overline{\nabla T}_s \cdot [-A_s \vec{j} - \hat{A}_s \vec{s}_s] + k_n \overline{\nabla T}_n \cdot [A_n \vec{j} - \hat{A}_n \vec{s}_n] + \\ & k_w \overline{\nabla T}_w \cdot [-A_w \vec{i} - \hat{A}_w \vec{s}_w] + k_e \overline{\nabla T}_e \cdot [A_e \vec{i} - \hat{A}_e \vec{s}_e] + \\ & \sum [\frac{\dot{Q}_{b,i}}{n_{F,i} A_{bF,i}} A_i] - h_a (T - T_a) A_a \end{aligned} \tag{4}$$

where the coefficients a, b, and c stand for first order (a=1, b=1, c=0) or second order (a=1.5, b=2, c=0.5) accuracy for the unsteady term.

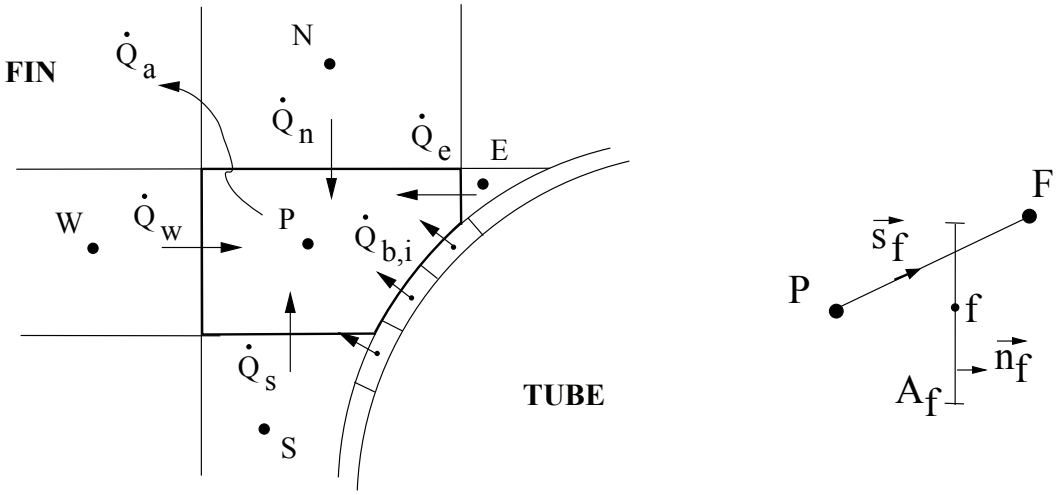

Figure 2: Fin control volume with main heat transfer interactions.

2.2 Tube discretized equations

Each tube within the finned tube bank has been solved numerically with a 2D (axial+angular directions) discretization (Figure 3). The thin fin hypothesis has been applied (uniform temperature in radial direction). The heat diffusion equation (Eq.1) has been applied to each control volume, considering the heat conduction interaction with tube neighbour nodes, the heat conduction to fin base, and the convective heat transfer from/to the air and refrigerant flows. The discretized equation is presented in Eq.6, where the temperature derivative with time has been solved again by a second order scheme.

$$\rho c_p \frac{aT_P - bT_P^0 + cT_P^{00}}{\Delta t} V = (\dot{Q}_s - \dot{Q}_n + \dot{Q}_w - \dot{Q}_e) + (\dot{Q}_i - \dot{Q}_a - \dot{Q}_b) \tag{5}$$

$$\begin{aligned} \rho c_p \frac{aT_P - bT_P^0 + cT_P^{00}}{\Delta t} V \;=\; & [(-k \frac{T_P - T_S}{\Delta z_S} A_s) - (-k \frac{T_N - T_P}{\Delta z_N} A_n) + (-k \frac{T_P - T_W}{\bar{r} \Delta \phi_W} A_w) - \\ & (-k \frac{T_E - T_P}{\bar{r} \Delta \phi_E} A_e)] + [h_i (T_i - T_P) A_i - h_a (T_P - T_a) A_a - \frac{T_P - T_b}{R_c} A_b] \end{aligned} \tag{6}$$

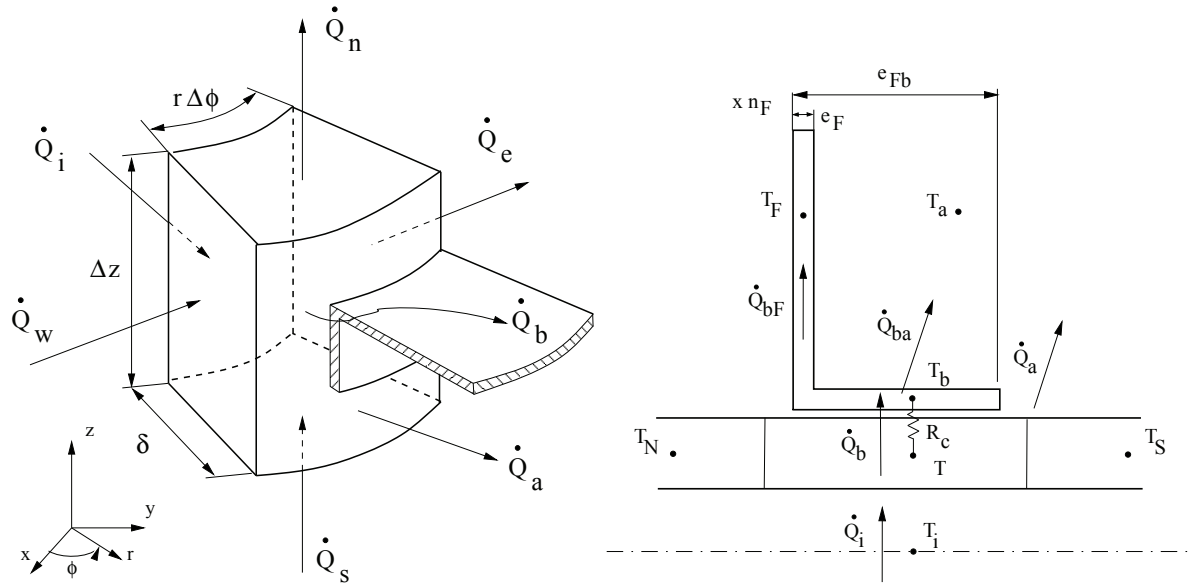

Figure 3: Tube control volume with main heat transfer interactions.

2.3 Tube-fin junction

In previous section, the formulation for the tube control volume has been stated referring to the heat transfer at the fin base by means of the contact thermal resistance to a fin base temperature T_b (Eq.6). This heat quantity is at the same time transferred from fin base to surrounding air and to the fin core, obtaining an additional equation (Eq.7). The relation to the fin core is presented in terms of temperature gradient. With this approach, the evaluation of the heat transfer to the fins is more accurate and better linked with fin temperature field. Combining both $\dot{Q}_b$ equations, the relation between fin temperature and liquid temperature can be obtained avoiding one additional calculation node at fin base (Eq.8).

$$\dot{Q}_b = \dot{Q}_{bF} + \dot{Q}_{ba} = -k(\nabla T|_b \cdot \vec{r})A_{bF} + h_a(T_b - T_a)A_{ba} \tag{7}$$

$$\dot{Q}_b = \frac{(T - T_a) - \frac{k(\nabla T|_b \cdot \vec{r})A_{bF}}{h_a A_{ba}}}{(\frac{R_c}{A_b} + \frac{1}{h_a A_{ba}})} \tag{8}$$

2.4 Gradient evaluation

The evaluation of the temperature gradients at fin cell centroids and at tube-fin base has been done by using the Least Squares technique, in accordance to (Pérez-Segarra et al., 2006a). If the temperature at each neighbor node "i" is estimated from current node "o" by a first-order extrapolation, an expression using the gradient at current node (desired value) is obtained: $T_i^* \approx T_o + \nabla T_o \cdot \vec{r}_{oi}$.
The minimisation of the sum of the squares ($S = \sum E_i^2$) of the differences between the calculated neighbor temperature and the estimated neighbor temperature ($E_i = T_i - T_i^*$) provides the desired gradient at current node. An important characteristic of this formulation is that the coefficients of the obtained system of equations are only dependent of the nodes position, therefore it is possible to pre-compute them and obtain important savings in computational time. Considering the final gradient expression (Eq. 9), the gradient dependent terms found in the fin and tube equations (heat diffusion at fin cell faces, heat transfer at the fin-tube junction) can be implicitly implemented in the matrix A of the system of equations.

$$\nabla T|_j = (\frac{\partial T}{\partial x}, \frac{\partial T}{\partial y})_j = (A_{x,j}T_j + \sum_{i=1}^{i=N} A_{x,i}T_i, A_{y,j}T_j + \sum_{i=1}^{i=N} A_{y,i}T_i) \tag{9}$$

For the evaluation of the gradient at fin cell centroids, the neighbor group of nodes has been established from fin cell neighbors plus the tube cell neighbors if the cell is in contact with the tube. For the evaluation of the gradient at the tube-fin contact, the tube cell "W" and "E" neighbors, the neighbor fin cells, and the neighbors of these fin cells have been included in the group of nodes where least squares technique is applied.

3. NUMERICAL ASPECTS

3.1 Method of Manufactured Solutions (MMS) - Analytical solution

At this code development stage, the Verification of the Code has been considered as a mandatory step in order to provide confidence into the new discretization method. The Method of Manufactured Solutions (MMS) (Roache, 2002) has been selected for this purpose. The basic idea of this method is to create an exact analytical solution, without considering its physical meaning. A source term is introduced in the equations, and it is used to generate a known solution. The comparison between the numerical calculated solution vs. the analytical one verifies the correctness of the code.
Focusing the problem on the case of a circular transversal fin in steady state and with constant thermal conductivity, and considering the convective heat transfer from the surrounding medium and internal heat generation, the differential heat diffusion equation can be written in cylindrical coordinates as:

$$\frac{d^2T}{dr^2} + \frac{1}{r}\frac{dT}{dr} - m^2(T - T_g) + \frac{\dot{q}_v}{k} = 0 \tag{10}$$

where $m^2 = (2h_a)/(ke_F)$. Introducing in this equation a manufactured solution (fixed by similarity to the solution of the straight fin of uniform cross section) as $\theta(r) = T - T_a = C_1 e^{mr} + C_2 e^{-mr}$, and applying boundary conditions ($\theta = \theta_i$ at fin-tube junction, and $\theta = 0$ at $r \to \infty$), the temperature equation is finally stated: $\theta(r) = \theta_i e^{m(r_i - r)}$. After fixing the temperature profile, the additional internal heat generation term is derived in order to accomplish the stated heat diffusion equation: $\dot{q}_v = \frac{km}{r}\theta_i e^{m((r_i - r)}$. This source term is implemented in the numerical code, and the boundary conditions of the computed domain are taken directly from the MMS temperature profile at the desired position.

3.2 Verification and numerical studies using MMS

The presented MMS has been taken as an analytical reference solution for code verification purposes. A baseline single rectangular steel fin (100x100 mm) around a circular tube (D_o=22mm) has been selected (m=$60m^{-1}$), from which fin parameter has been changed to consider a wide range of temperature profiles at tube base. The tube base and the surrounding air temperatures have been fixed, while the temperatures at the boundaries and the internal heat generation have been determined from previous analytical expressions. The obtained results show, for all the numerical approaches, a very good agreement between the code and the exact analytical MMS solution, for both the temperatures and the heat transferred to the surrounding air (Figure 4). The blocking-off shows a mean error (error = $100|T - T_{MMS}|/|T_i - T_a|$) lower than 0.1% for a grid with $N_f > 30$, and achieves errors of 0.02% with higher fin grid densities. The new cutting cell method provides an error lower than 0.1% for $N_f > 10$, and shows an one-order of magnitude lower error (0.002%) with higher densities. This improvement in grid behaviour at fin-tube junction strongly reduces the necessary mesh and the corresponding computational resources. The influence of the tube angular mesh is only reflected for high fin densities and within a very low error band (0.001-0.004%), showing a trend to improve results with higher tube densities.
Another aspect that has been studied is the fin grid density at inter tube zones in relation with the fin grid density around the tubes . This relation (K_f) has been changed from 1 to 4 (baseline case: cutting cell with $N_f = 40$ and $N_{ang} = 60$), obtaining an increment of the error from 0.002% to 0.04%.
Finally, as commented before, the fin parameter (m) has also been changed (baseline case: cutting cell with $N_f = 40$ and $N_{ang} = 60$) in order to assure the goodness of the method for a wide range of temperature profiles at fin-tube junction. While for $20 < m < 80$ the error is maintained at very low values ($< 0.005\%$), for $80 < m < 190$ the error smoothly increase up to error values of 0.01%.

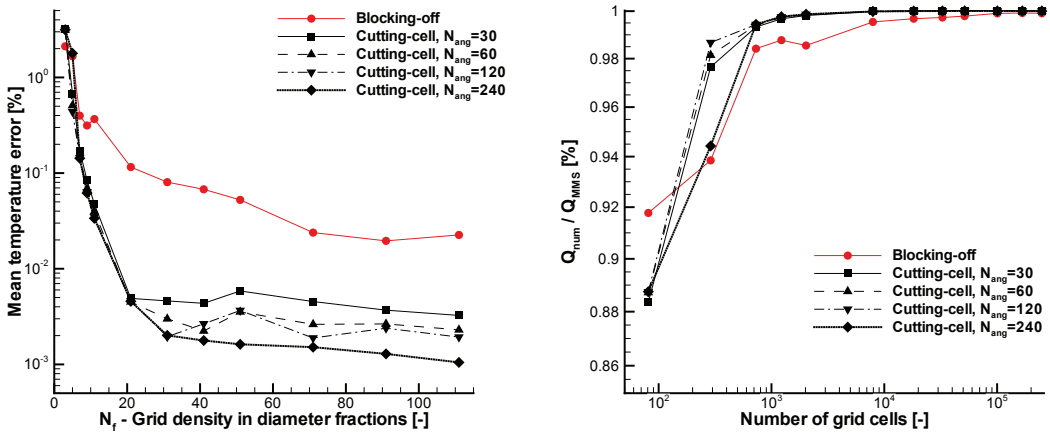

Figure 4: Comparison between discretisation methods.

3.3 Solvers of the set of equations

Another action to reduce the computational resources needed is to change the solver of the system of equations. The selected strategy has been, when possible, to maintain the matrix of coefficients constant and equal for all the fin levels. The difference between the current coefficients and the constant estimation would go into the source term. Having the matrix of the coefficients constant, advanced direct linear solvers can be applied. Considering the low density of the matrix, sparse matrix oriented solvers have been selected: for symmetric matrices Cholesky solver, and for non-symmetric a sparse LU solver (Davis, 2004). This strategy has allowed to compute in a single desktop computer grids up to 250000 cells.

4. ILLUSTRATIVE RESULTS

4.1 Evaporator solid core transient simulation

After the presentation and verification of the new model for the transient evaluation of the fin-and-tube solid core, it is of interest presenting an illustrative result of a transient case. The selected example is representative of a refrigeration fin (Figure 5). A preliminary test is briefly presented which reproduces a cooling/heating process, analogous to a hot-gas defrosting operation (without frosting/melting process): first the evaporation process cools the tube-fin elements, then a hot-gas flow with higher temperature and lower heat transfer coefficients start to heat the exchanger, and finally the liquid+vapor mixture again cools the fin-tube surfaces.

4.2 Stratified evaporating flow; dry vs. wet heat transfer coefficient

Another interesting aspect that configures the new methodology is the angular discretisation of the tubes. As a first study, a typical air cooled evaporator under liquid overfeed conditions has been simulated, having 50% in-tube surface (bottom) liquid and 50% surface (top) vapor. The heat transfer coefficient ratio between liquid and vapor has been changed from 1 to 200, maintaining the mean heat transfer coefficient (Figure 6). In this way, the effect of angular heat coefficient variation is analysed for this case; from unity up to ratios of 50 the effect is notorious, while for higher values it has almost no effect.

5. CONCLUSIONS

A novel modelling technique for the transient simulation of the fin-and-tube heat exchanger solid core, based on a cutting-cell discretization approach, has been presented throughout the paper. A very detailed

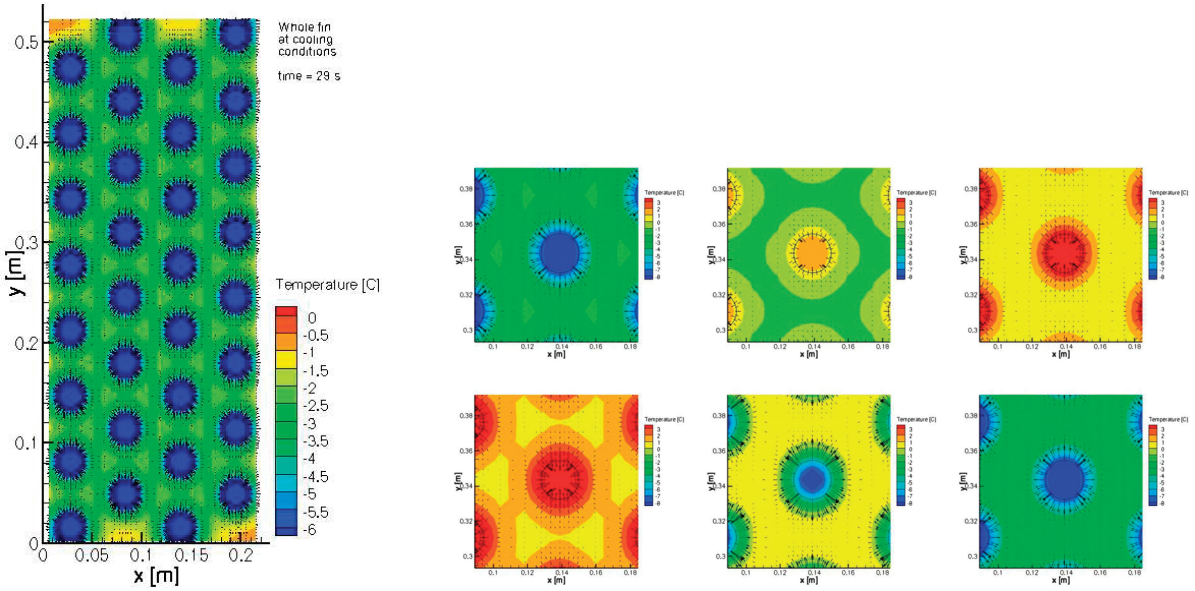

Figure 5: Full transient continuous fin simulation. Detailed view around a tube, for different time steps.

presentation of the mathematical background is provided, emphasizing the linkage of the tubes and fins through the temperature gradient at fin base. The numerical aspects such as the discretization and the solvers used are also given. A verification of the code is also shown, based on the MMS method, obtaining accurate results. Finally, two illustrative application cases are briefly presented, one for the transient simulation of the fin, and the second for the influence of non-uniform in-tube heat transfer coefficients. From the authors point of view, the proposed approach is an interesting contribution to achieve not only steady state but also a full-transient fin-and-tube heat exchanger modelling.

NOMENCLATURE

A	Area, gradient coefficient	(m^2),(-)	**Subscripts**	
a,b,c	components of second order scheme	(-)	a	air-side
c_p	heat capacity at constant pressure	(J/kgK)	ang	angular
d	distance	(m)	b	fin-tube junction
e	thickness	(m)	conv	convective
E	least squares temperature error	(K)	F	fin,neighbour point
h	convective heat transfer coefficient	(W/m^2K)	f	face
m	fin parameter	$(1/m)$	i	liquid-side, inner
N,n	number	(-)	P	central point
$\vec{n}$	surface unit vector	(-)		
$\dot{q}$	heat flux	(W/m^2)	**Greek**	
$\dot{Q}$	heat rate	(W)	ρ	density (kg/m^3)
R	thermal contact resistance	(m^2K/W)	θ	temperature difference (K)
r	radius	(m)		
S	sum of error squares	(K^2)		
$\vec{s}$	direction unit vector	(-)		
T	temperature	(K)		
t	time	(s)		
V	volume	(m^3)		

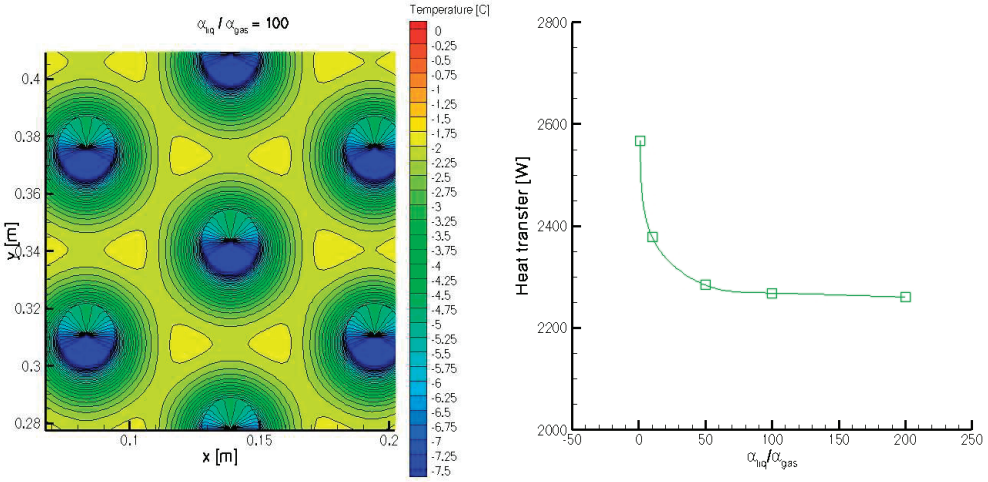

Figure 6: Detail of fin temperature map for $\alpha_{liq}/\alpha_{gas} = 100$. Influence of heat transfer coefficient ratio.

REFERENCES

Davis, T. A., 2004, Algorithm 832: UMFPACK V4.3—an unsymmetric-pattern multifrontal method, *ACM Transactions on Mathematical Software*, 30, no. 2:p. 196–199.

Hoffenbecker, N., Klein, S. A., and Reindl, D. T., 2005, Hot gas defrost model development and validation, *International Journal of Refrigeration*, 28, no. 54:p. 605–615.

Liang, S. Y., Wong, T. N., and Nathan, G. K., 2000, Comparison of one-dimensional and two-dimensional models for wet-surface fin efficiency of a plate-fin-tube heat exchanger, *Applied Thermal Engineering*, 20, no. 10:p. 941–962.

Oliet, C., Pérez-Segarra, C. D., Danov, S., and Oliva, A., 2002, Numerical simulation of dehumidifying fin-and-tube heat exchangers. model strategies and experimental comparisons, *Proceedings of the 2002 International Refrigeration Engineering Conference at Purdue*, CD-ROM ref. R5-5, 8 p.

Pérez-Segarra, C., Farré, C., Cadafalch, J., and Oliva, A., 2006a, Analysis of different numerical schemes for the resolution of convection - diffusion equations using finite volume methods on three dimensional unstructured grids. Part I: Discretization schemes., *Numerical Heat Transfer, Part B*, 49, no. 4:p. 333–350.

Pérez-Segarra, C. D., Oliet, C., and Oliva, A., 2006b, Thermal and Fluid Dynamic Simulation of Automotive Fin-and-Tube Heat Exchangers. Part 1: Mathematical Model, *Heat Transfer Engineering*, 29, no. 5:p. 484–494.

Roache, P. J., 2002, Code Verification by the Method of Manufactured Solutions, *Journal of Fluids Engineering*, 124, no. 1:p. 4–10.

Sommers, A. D. and Jacobi, A. M., 2006, An exact solution to steady heat conduction in a two-dimensional annulus on a one-dimensional fin: application to frosted heat exchangers with round tubes, *International Journal of Refrigeration*, 128, no. 4:p. 397–404.

ACKNOWLEDGEMENTS

This research work has been partially funded by the 'Ministerio de Educación y Ciencia, Secretaria de Estado de Universidades e Investigación', Spain (refs. ENE2005-08302, ENE2006-11099).